DOI: 10.1002/adma.200700942

Sculptured Layer-by-Layer Films**

By *Yen-Hsi Lin*, *Chaoyang Jiang*, *Jun Xu*, *Zhiqun Lin*,* and *Vladimir V. Tsukruk**

The precise assembly of nanostructured materials into two (2D) and three-dimensional (3D) periodic microscopic arrays is achieved by employing various assembling technologies such as microparticle self-organization,[1] photolithography,[2] holographic lithography,[3] selective chemical etching,[4] ink printing,[5] laser-based polymerization,[6] selective responsive grafting,[7] and inversion of bilayers.[8] Soft lithography, such as microcontact printing has been widely applied to tackle this challenge in a few steps, with a submicrometer resolution, and at low cost.[9–11] It has been demonstrated that the most popular fabrication of well-defined nanostructured materials with layer-by-layer (LbL) assembly can be combined with photolithography and microprinting to fabricate complex 2D and 3D structures with modulated distribution of different components.[12–14] Examples of the micropatterned assembly of nanoparticles, microchannels, antireflective coatings, and Raman arrays have already reported.[15–20] A variety of functional materials have been utilized in the LbL construction to make these structures suitable for prospective applications as antiwetting coatings, sensitive films for solar cells, fuel cells, ultra-strong nanomaterials, microcapsules, and membranes for controlled drug release.[21–27] On the other hand, microstructural arrays based upon the principles of either diffraction or refraction with in-printed microscopic modulations are extensively used as optical components such as grating, beam splitters, microlenses, displays, and mirrors.[28–31]

A vast majority of LbL structures have been fabricated on solid planar or curved (microparticle) supports and represent essentially 2D planar structures with vertical (along the surface normal) modulations of chemical composition. Micropatterning of LbL films has been recently reviewed by Hammond.[32] Few examples of free-standing LbL structures have been reported either in the form of uniform, micropatterned, or curved shell structures.[33–37] Therefore, although potential for the fabrication of interesting modulated structures, which provides for optical effects, is inherently present in the LbL technology, few attempts have been made to investigate the feasibility of the fabrication of modulated LbL structures for light control. For example, in a recent study, Rubner et al. have demonstrated that a properly matched LbL coating can serve for constructive–destructive light interferences with efficient antireflective ability.[18,38] In a related study, Rubner and Cohen have demonstrated that a proper modulation of the reflective index within LBL films might lead to a pronounced structural color effect with selective reflection of visible light controlled by the reflective index modulation rather than the presence of conjugated molecules with proper electronic structures.[39] Although these initial studies showed some potential in LbL technology to generate nanostructured materials with the ability to control visible light diffraction/reflection, they have been limited to one-dimensional modulation of the refractive properties.

In this communication, an example of 3D LbL grating structures with the ability to diffract light because of the modulation of local LbL film shape with microscopic periodicity and nanometer-scale vertical modulations is reported. In these freely suspended 3D LbL films, the effective modulation of the refractive properties is caused by the topological variation of the local film shape, thus representing a purely structural color effect. A simple and economical spin-assisted LbL assembly of conjugated polyelectrolytes on a sacrificial microimprinted modulated substrate was employed here to generate a robust, free-standing sculptured LbL structure with an effective thickness of 60 nm and a 160 nm peak-to-peak vertical modulation on a square lattice with 2.5 μm lateral periodicity (Figure 1). These films demonstrate efficient optical grating properties and bright structural colors in a reflective mode controlled by the in-plane spacing and the angle of incidence.

The conjugated polyelectrolyte, poly(2,5-methoxypropyloxy sulfonate phenylene vinylene) (MPS-PPV) applied in the LbL assembly synthesized here was critical in providing a mechanically strong structure as has been tested in our previous work to fabricate mechanically robust planar ultrathin LbL films.[40] MPS-PPV is a well known water-soluble conjugated polymer with a highly charged, stiff backbone and strong fluorescence properties.[26] Planar LbL films of MPS-PPV and poly(allylamine hydrochloride) (PAH) demonstrate excellent mechanical properties combined with high fluorescence as has been demonstrated in our previous work.[40]

[*] Prof. V. V. Tsukruk, Y.-H. Lin, Dr. C. Jiang
School of Materials Science and Engineering
Georgia Institute of Technology
Atlanta, Georgia 30332 (USA)
E-mail: vladimir@mse.gatech.edu
Prof. Z. Lin, Y.-H. Lin, J. Xu
Department of Materials Science and Engineering
Iowa State University
Ames, Iowa 50011 (USA)

[**] This work was supported by the AFOSR, FA9550-05-1-0209 and NSF-CBET-0650705 grants, and the 3M Non-tenured Faculty Award (ZL). JX thanks the Institute for Physical Research and Technology of Iowa State University for a Catron graduate research fellowship. The authors also thank T. M. Pepper and O. Ugurlu for SEM images, and H. Ko and E. Merrick for assistance with sample preparation. Supporting Information is available online at Wiley InterScience or from the author.

ADVANCED MATERIALS

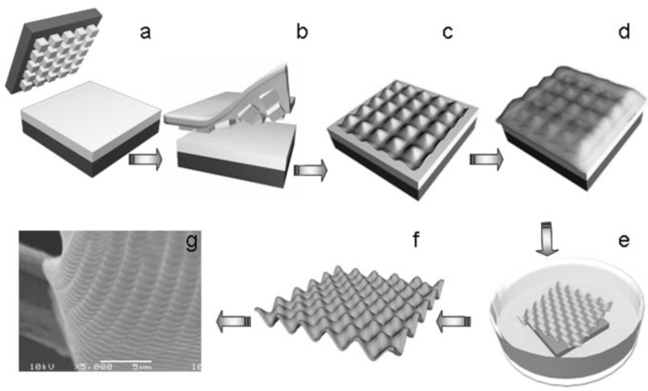

Figure 1. Schematic illustration of the route for the fabrication of sculptured LbL films by combining microstamping and sacrificial templates and scanning electron microscopy (SEM) image of the freely suspended LbL film with a square pattern. a) Preparation of a layer of sacrificial PS micropattern on the stamp; b) microcontact printing onto a flat PS film; c) formation of a micropatterned PS sacrificial template; d) spin-assisted LbL deposition; e) release of sculptured LbL film by dissolving sacrificial PS micropattern; f) 3D schematic of sculptured LbL film; and g) SEM image of the freely suspended sculptured LbL film.

To fabricate sculptured LbL films, a modified experimental procedure was employed, which includes the use of a micropatterned modulated sacrificial substrate (Figure 1). A sacrificial polystyrene (PS) micropatterned template was first obtained by using capillary transfer microprinting as described in a previous publication.[34] The LbL film was fabricated on this substrate and released to form a free-standing sculptured film with dimensions of about 3 mm × 3 mm and a clearly seen square micropattern that extended over a large surface area (Figure 1, see experimental).[33] By using this approach, it is also possible to fabricate freely suspended LbL sculptures with different patterns that range from several micrometers to hundreds of micrometers (see supporting information) but here only one type of squared sculptured LbL film is discussed in detail.

An atomic force microscopy (AFM) topographical image demonstrates the square lattice on a poly(dimethylsiloxane) (PDMS) stamp that was exploited to form the micropatterned sacrificial substrate (Figure 2a). The spacing in this sacrificial micropattern is 2.4 µm with a diagonal distance of 3.4 µm and a 400 nm difference in elevations. AFM imaging of the freely sculptured LbL film released from the substrate, conducted in a light tapping mode on both sides of the film, revealed a topographical 3D replica of the original micropatterned substrate with the periodicity of the lateral modulation identical (within experimental error) to that in the original microstamp (see topography of both sides and corresponding cross-sections in Figures 2b–d). Apparently, the 3D structure of the sacrificial micropatterned PS template have been successfully imprinted into the 3D topology of the nanometer-scale LbL film with a 'nominal' thickness of about 60 nm with the original square shape of the template somewhat smeared during assembly (Figure 2c).

The overall 'thickness' (peak-to-peak value) of the sculptured 3D LbL film reached 160 nm, which is smaller than the elevation difference in the original template and indicates some contraction in the process of drying and transfer. Although AFM images of the top and bottom surfaces display a modulated shape of the LbL film with 'imprinted' periodicity, the difference in the cross-sectional shape suggests an asymmetric morphology (Figure 2e). The bottom side of the LbL film, which was in contact with the micropatterned sacrificial layer, has a difference in elevations of 125 nm while the top side of film shows a smaller difference of 55 nm (Figure 2d). It is believed that this difference between the two sides of the freestanding film is a result of the relatively small channel length of the micropatterned PS sacrificial layer, and it might also be related to the features of the array processing such as uneven water access because of the surface topography during LbL assembly.

The optical and fluorescence images of the sculptured LbL film suspended on the transmission electron microscopy (TEM) grid or across the 150 µm round opening within a copper holder showed large defect-free areas with a clearly visible imprinted square lattice (Figures 3 and 4). The fluorescence of the MPS-PPV observed in solution is preserved in this state as confirmed by photoluminescence spectroscopy (inset in Figure 3b). Green fluorescence with an emission maximum at 530 nm, which is blue-shifted, is similar to that observed for planar LbL films (see earlier discussion on planar MPS-PPV LbL films, Ref. [40]). Pieces of a damaged sculptured LbL film showed very regular fracturing with straight cracks that always propagated along the lattice sides and changed a register in a 'quantified' manner with an integer number of squared cells (Figure 3c). This type of 'organized' brittle fracture under high stresses has been reported for 3D ordered microporous solids fabricated with interference lithography and has been associated with the preferential crack propagation along 'weak lines' in the lattices.[3] Higher magnification of the fractured sculptured LbL film showed a regular pattern on two sides of the 3D array with a characteristic smeared-squared shape of the individual cells as discussed above (Figures 2c and 3d).

Micromechanical properties of sculptured LbL films have been tested under both compressive and tensile modes in accordance with the usual procedures discussed earlier.[41–44] The film deflection under a hydrostatic pressure applied from one side is shown in Figure 4b in comparison with a conventional planar LbL film with identical composition. The sculptured LbL films showed a much higher deflection, which indicates a less stiff response, associated with the modulated 3D shape of the polymer film. In fact, the effective elastic modulus of this structure, obtained from the data analysis, was calculated to be within 0.4 ± 0.1 GPa, which is an order smaller than that found earlier for a planar MPS-PPV LbL film.[40] This value of the elastic modulus is a characteristic of tough rubbery polymers rather than conjugated polymers in the glassy state. Such a significant difference implies very different mechanisms of the elastic deformation for planar and

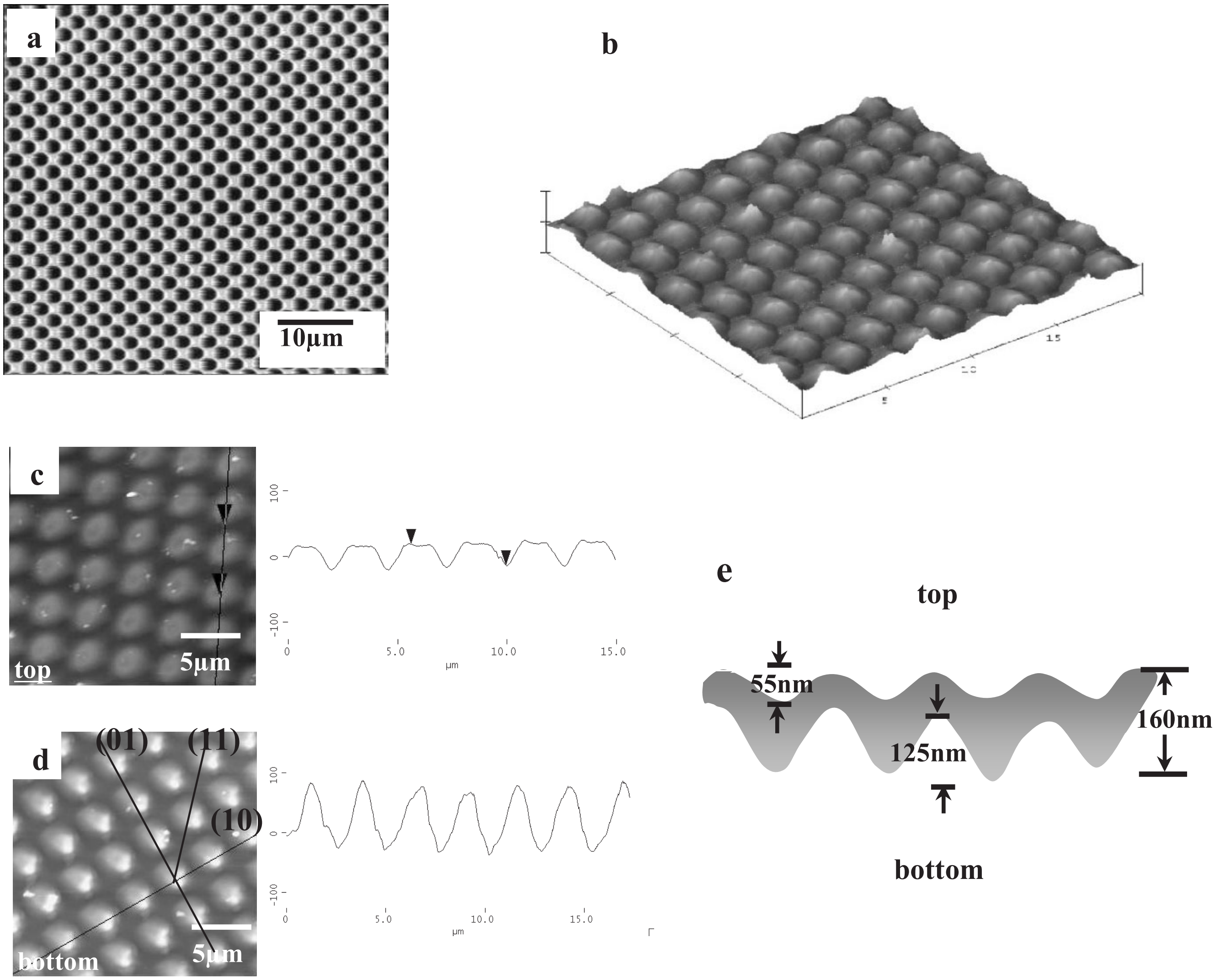

Figure 2. a) AFM image of the PDMS stamp used for capillary transfer. b) AFM 3D surface plot of released LbL film; AFM line profile analysis of c) top and d) bottom of a freely standing sculptured LbL film on a TEM grid. e) Schematics of 3D LbL film with major dimensions.

sculptured films within a strain range below 0.5 %. It is suggested that an expansion ('unfolding') of the 3D modulated structure occurs in sculptured LbL films in contrast to the ordinary tensile deformation of conjugated backbones in the planar film. Moreover, very low resistance under tensile stress has also been confirmed with the film compression.[45] For this test, the sculptured LbL film was transferred to a PDMS substrate and compressed by 0.1–0.5 % until a periodic buckling pattern appeared (Figure 4c). The spacing of these wrinkles, as determined from optical micrographs, was 3.6 ± 0.2 μm as obtained from Fourier transformations (Figure 4d). This periodicity corresponds to an elastic modulus of 0.30 ± 0.03 GPa, which is close to that measured from tensile deformation.[46] A slight difference between the results of compression and tensile might be a result of the simple model that was utilized in the buckling data analysis. It is interesting to note that this spacing corresponds to the 'diagonal' direction in the square lattice of the modulated areas and, thus, the collapse of the squared lattice under compression occurs along the direction that includes the widest gap between modulations (between next-next neighbors), which is in contrast to tensile deformation in which unfolding occurs along grooves between next neighbors (Figure 2d). Therefore, the symmetry of the sculptured structure defines the preferential fracturing direction along the rows of modulated areas under tensile stress ((01) and (10) directions) but different (11) direction (at angle 45°) for a collapsed film under compressive stress (Figure 2d).

Finally, bright coloration in a reflection mode was observed for a sculptured LbL film transferred onto a silicon wafer in contrast to planar LB films, which show a weak brownish color because of absorption of conjugated backbones.[40] Our experiments showed that white light can be reflected by a sculptured LbL film with the intense color changing from blue to red while adjusting the view angle (Figure 5a). The intensity of the color is remarkable considering that the physical thickness of the LbL film is only 60 nm. Correspondingly, the 2D

ADVANCED MATERIALS

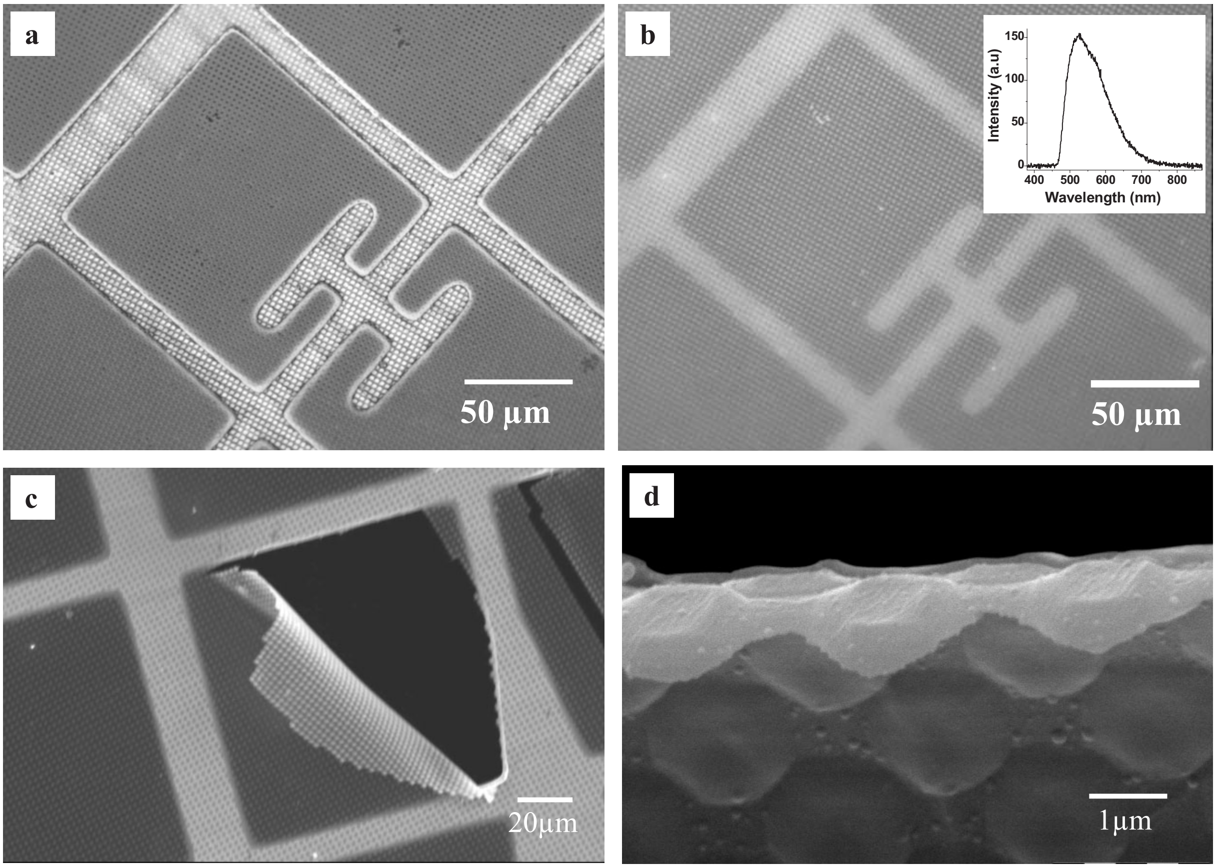

Figure 3. Sculptured LbL film on TEM grid: a) optical image, b) fluorescence image with fluorescence spectrum (inset), c) SEM image of the damaged piece of the 3D LbL film with characteristic fracturing (top view), d) high-resolution SEM image of freely standing 3D LbL film (side view).

diffraction pattern has been observed under an incident illumination from a He–Ne laser ($\lambda = 632$ nm). Bright diffraction spots that form a square lattice can be seen beyond the third order (Figure 5b). The diffraction pattern produced by the 3D LbL film should follow a Fraunhofer law with positions of individual spots in a reciprocal space defined by the symmetry and spacing of the modulations in real space.[47] Thus, from multiple diffraction orders (m) the expected distribution of the diffraction spots is estimated taking into account the known spacing of the square modulations of 2.4 µm. Under this assumption, excellent coincidence was observed between the experimental positions measured and those estimated from the spacing of the shape modulation as demonstrated for the (01) direction in Figure 5c.

The modulated refractive properties achieved by the topological variation of the sculptured LbL film shape can generate an intense structural color effect with bright structural colors and optical grating properties, a phenomenon that is of interest for light-controlling polymeric microdevices. Overall, this study shows an interesting potential in LbL technology to generate optically relevant 3D nanostructured materials with the ability to control visible light diffraction beyond one-dimensional modulation of the refractive properties reported previously.

Experimental

Poly(allylamine hydrochloride) (PAH, MW = 65 000) was purchased from Aldrich and used as received. The water-soluble conjugated polymer MPS-PPV was synthesized according to the known routine as described before [40,48]. The (100) silicon wafers with a typical size of 10 mm × 20 mm were cleaned in piranha solution (3 : 1 mixture of H_2SO_4/H_2O_2) for 1 h and then rinsed thoroughly with Nanopure water (resistivity 18 MΩ cm). PDMS stamps were prepared by curing liquid prepolymer (Sylgard 184, Dow Chemical) on top of a corresponding silicon master (Mikromasch) at 60 °C for 1 h in a vacuum oven.

The experimental procedure for fabricating a 3D sculptured LbL film was conducted under usual laboratory conditions with relative humidity of ~40 %. (Figure 1). First, a layer of a sacrificial PS film (MW = 200 000, 2 % in toluene) was spin cast (3000 rpm for 20 s) on a silicon wafer and a second layer of sacrificial PS micropattern was fabricated by using capillary transfer lithography [33]. For this procedure, the PDMS stamp was soaked in toluene for 1–2 min and brought into conformal contact with the PS film on the PDMS substrate and pressed for 1 min. When the PDMS stamp was detached, the PS material was trapped inside the recessed regions of the PDMS stamp. The polymer pattern formed in this way was then immediately transferred onto the first sacrificial PS layer by conformal contact of the PDMS stamp for 1 min [33]. Tetrahydrofuran (THF) was used to dissolve the sacrificial PS layer in order to release the films. The polymer films with different thicknesses were fabricated using a spin-assisted LbL (SA-LbL) method as described in detail in previous publications [33,36]. A droplet (150 µL) of 0.2 % (w/w) MPS-PPV and PAH layers

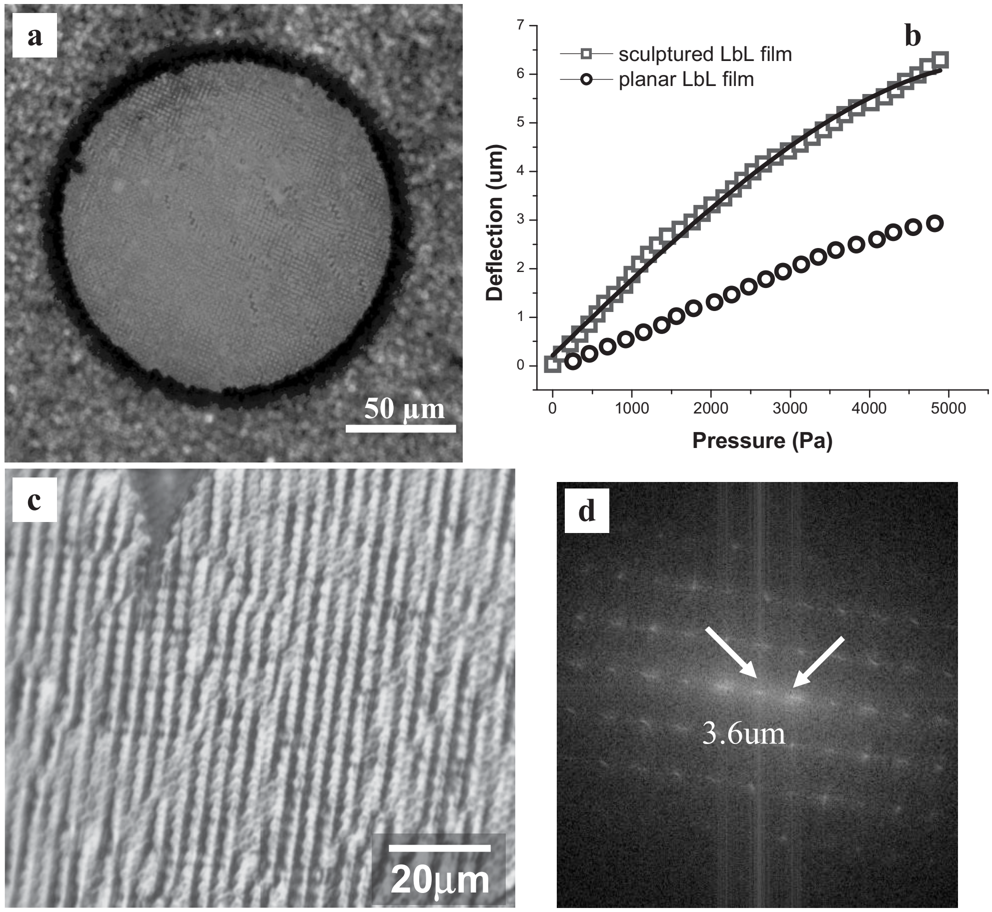

Figure 4. Sculptured LbL film suspended across an opening into a copper holder (a). Mechanical tests: bulging test for sculptured and planar LbL films, solid line shows theoretical fit (b); buckling pattern (c), and corresponding 2D fast Fourier transform (d) for a compressed 3D LbL film.

were deposited in an alternating manner. This procedure was repeated until the needed 25 polymer bilayers. The LbL film presented here in detail has a general formula $(MPS\text{-}PPV/PAH)_{25}$.

The LbL films were transferred to Nanopure water where they could then be picked up with different substrates such as a highly polished copper plate with a single micromachined hole, a TEM grid with index finer (Ted Pella, Inc), or a silicon wafer with and without holes. AFM scanning was conducted on a Dimension 3000-Nanoscope IIIa microscope (Digital Instruments) according to the usual procedure [49,50]. The film thickness was obtained with AFM scans along the film edge. The photoluminescence image and spectrum were taken with a Leica DM 4000 microscope with a mercury source and attached CRAIG QDI202 microscopic spectrophotometer. The samples were excited at 365 nm and the emission spectra were collected within 400–1000 nm. Scanning electron microscopy (SEM) was conducted in secondary electron scattering mode at 5 keV (JEOL JSM-6060 LV and JEOL 5800 LV). The bulging test was conducted by applying a hydrostatic pressure to one side of an LbL film that covered a copper plate with 150 μm holes in accordance with the usual procedure under ambient conditions [37]. The film deflection was measured using a custom-built interference optical set-up with a He–Ne laser and the elastic modulus was calculated as described earlier [51]. The experimental data was analyzed by using an appropriate equation for elastic membrane deformation as discussed in detail elsewhere [51]. At least five different specimens with the same composition were tested. The buckling instability was observed for the film transferred to the PDMS substrate and the buckling pattern formed under compressive stress was analyzed according to a known procedure [41,42].

Received: April 19, 2007
Revised: May 29, 2007
Published online: October 30, 2007

[1] M. H. Lu, Y. Zhang, *Adv. Mater.* **2006**, *18*, 3094.
[2] S. Y. Lin, J. G. Fleming, *Nature* **1998**, *394*, 251.
[3] J.-H. Jang, C. K. Ullal, T. Choi, M. C. Lemieux, V. V. Tsukruk, E. L. Thomas, *Adv. Mater.* **2006**, *18*, 2123.
[4] S. Noda, K. Tomoda, N. Yamamoto, A. Chutinan, *Science* **2000**, *289*, 604.
[5] G. M. Gratson, M. Xu, J. A. Lewis, *Nature* **2004**, *428,* 386.
[6] M. Campbell, D. N. Sharp, M. T. Harrison, R. G. Denning, A. J. Turberfield, *Nature* **2000**, *404*, 53.
[7] a) I. Luzinov, S. Minko, V. V. Tsukruk, *Prog. Polym. Sci.* **2004**, *29*, 635. b) V. V. Tsukruk, *Prog. Polym. Sci.* **1997***, 22*, 247.
[8] J. Léopoldès, P. Damman, *Nat. Mater.* **2006**, *5*, 957.
[9] a) E. Kim, Y. Xia, G. M. Whitesides, *Nature* **1995**, *376*, 581. b) J. Zaumseil, M. A. Meitl, J. W. P. Hsu, B. R. Acharya, K. W. Baldwin, Y. -L. Loo, J. A. Rogers, *Nano Lett.* **2003**, *3*, 1223.
[10] G. M. Whitesides, E. Ostuni, S. Takayama, X. Y. Jiang, D. E. Ingber, *Ann. Rev. Biomed. Eng.* **2001**, *3*, 335.
[11] K. Y. Suh, Y. S. Kim, H. H. Lee, *Adv. Mater.* **2001**, *13*, 1386.

ADVANCED MATERIALS

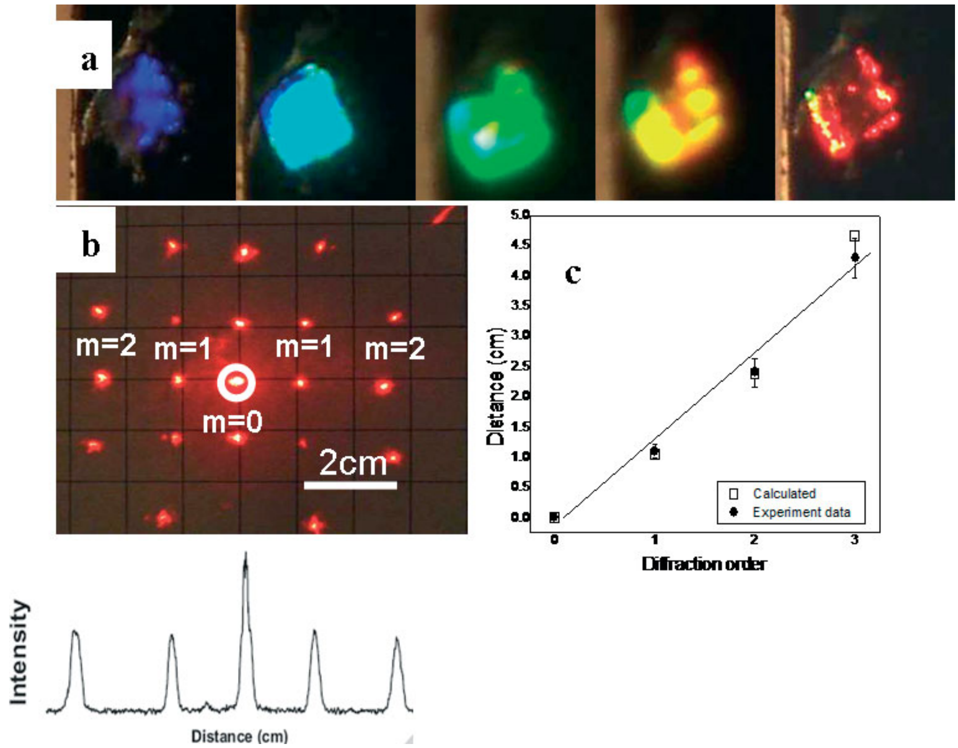

Figure 5. a) Sculptured LbL film with different structural colors generated at different viewing angles. b) The diffraction pattern produced by the LbL film in the reflection mode with intensity versus distance profiles. c) The calculated and experimental positions of diffraction spots of different orders along the (01) direction.

[12] M. Mrksich, *Chem. Soc. Rev.* **2000**, *29*, 267.
[13] G. Roberts, Ed, *Langmuir–Blodgett Films* Kluwer Academic, Norwell MA **1990**.
[14] G. Decher, *Science* **1997**, *277*, 1232.
[15] J. Park, L. D. Fouche, P. T. Hammond, *Adv. Mater.* **2005**, *17*, 2575.
[16] C. Jiang, S. Markutsya, V. V. Tsukruk, *Langmuir* **2004**, *20*, 882.
[17] C. Jiang, H. Ko, V. V. Tsukruk. *Adv. Mater.* **2005**, *17*, 2127.
[18] J. A. Hiller, J. D. Mendelsohn, M. F. Rubner, *Nat. Mater.* **2002**, *1*, 59.
[19] F. Hua, T. Cui, Y. M. Lvov, *Nano Lett.* **2004**, *4*, 823.
[20] C. Jiang, V. V. Tsukruk, *Adv. Mater.* **2006**, *18*, 829.
[21] L. Zhai, M. C. Berg, F. C. Cebeci, Y. Kim, J. M. Milwid, M. F. Rubner, R. E. Cohen, *Nano Lett.* **2006**, *6*, 1213.
[22] C. Jiang, S. Markutsya, Y. Pikus, V. V. Tsukruk, *Nat. Mater.* **2004**, *3*, 721.
[23] A. G. Agrios, I. Cesar, P. Comte, M. K. Nazeeruddin, M. Grätzel, *Chem. Mater.* **2006**, *18*, 5395.
[24] Z. Tang, N. A. Kotov, S. Magonov, B. Ozturk, *Nat. Mater.* **2003**, *2*, 413.
[25] D. N. Lynn, *Soft Matter* **2006**, *2*, 269.
[26] a) A. G. Skirtach, C. Dejungnat, D. Braun, A. S. Susha, A. L. Rogach, W. J. Parak, H. Möhwald, G. B. Sukhorukov, *Nano Lett.* **2005**, *5*, 1371. b) F. Caruso, *Adv. Mater.* **2001**, *13*, 11.
[27] J. W. Baur, S. Kim, P. B. Balanda, J. R. Reynolds, M. F. Rubner, *Adv. Mater.* **1998**, *10*, 1452.
[28] J. Kim, M. J. Serpe, L. A. Lyon, *Angew. Chem. Int. Ed.* **2005**, *44*, 1333.
[29] J.-Y. Ha, D.-Y. Jeong, J.-S. Kim, S.-J. Yoon, *J. Opt. A: Pure Appl. Opt.* **2007**, *9*, 170.
[30] M. Wu, T. W. Odom, G. M. Whitesides, *Adv. Mater.* **2002**, *14*, 1213.
[31] K.-H. Jeong, J. Kim, L. P. Lee, *Science* **2006**, *312*, 557.
[32] P. T. Hammond, *Adv. Mater.* **2004**, *16*, 1271.
[33] A. Mamedov, N. A. Kotov, *Langmuir* **2000**, *16*, 5530.
[34] H. Ko, C. Jiang, V. V. Tsukruk, *Chem. Mater.* **2005**, *17*, 5489.
[35] C. Jiang, K. Wang, R. Gunawidjaja, Y.-H. Lin, M. K. Grupta, D. L. Kaplan, R. R. Naik, V. V. Tsukruk, *Adv. Funct. Mater* **2007**, *17*, 2229.
[36] C. Jiang, S. Markutsya, H. Shulha, V. V. Tsukruk, *Adv. Mater.* **2005**, *17*, 1669.
[37] C. Jiang, S. Markutsya, V. V. Tsukruk, *Adv. Mater.* **2004**, *16*, 157.
[38] Z. Wu, J. Walish, A. Nolte, L. Zhai, R. E. Cohen, M. F. Rubner, *Adv. Mater.* **2006**, *18,* 2699.
[39] Z. Wu, D. Lee, M. F. Rubner, R. E. Cohen, *Small* **2007**, *3*, 1445.
[40] Y.-H. Lin, C. Jiang, J. Xu, Z. Lin, V. V. Tsukruk, *Soft Matter* **2007**, *3*, 432.
[41] A. J. Nolte, M. F. Rubner, R. E. Cohen, *Macromolecules* **2005**, *38*, 5367.
[42] C. Jiang, S. Singamaneni, E. Merrick, V. V. Tsukruk, *Nano Lett.* **2006**, *6*, 2254.
[43] S. Jayaraman, R. L. Edwards, K. J. Hemker, *J. Mater. Res.* **1999**, *14*, 688.
[44] C. Poilane, P. Delobelle, C. Lexcellent, S. Hayashi, H. Tobushi, *Thin Solid Films* **2000**, *379*, 156.
[45] C. M. Stafford, C. Harrison, K. L. Beers, A. R. Karim, E. J. Amis, M. R. VanLandingham, H.-C. Kim, W. Volksen, R. D. Miller, E. E. Simonyi, *Nat. Mater.* **2004**, *3*, 545.
[46] A. L. Volynskii, S. Bazhenov, O. V. Lebedeva, N. F. Bakeev, *J. Mater. Sci.* **2000**, *35*, 547.
[47] D. Winoto, S. H. Carr, *Macromolecules* **1996**, *29*, 5149.
[48] A. D. Smith, C. K. F. Shen, S. T. Roberts, R. Helgeson, B. J. Schwartz, *Res. Chem. Intermed.* **2007**, *33*, 125.
[49] V. V. Tsukruk, D. H. Reneker, *Polymer* **1995**, *36*, 1791.
[50] V. V. Tsukruk, *Rubber Chem. Technol.* **1997**, *70*, 430.
[51] S. Markutsya, C. Jiang, Y. Pikus, V. V. Tsukruk, *Adv. Funct. Mater.* **2005**, *15*, 771.

